

# Fluorescent Nanorods and Nanospheres for Real-Time In Vivo Probing of Nanoparticle Shape-Dependent Tumor Penetration\*\*

Vikash P. Chauhan, Zoran Popović, Ou Chen, Jian Cui, Dai Fukumura, Mounji G. Bawendi,\* and Rakesh K. Jain\*

Nanomedicine has offered new hope for cancer treatment.<sup>[1]</sup> Nanotherapeutics exhibit many advantages over small-molecule chemotherapeutics, including diminished systemic toxicity and improved circulation times. Unfortunately, non-uniformly leaky vasculature<sup>[2]</sup> and a dense interstitial structure<sup>[3]</sup> hinder their effective delivery to tumors.<sup>[4]</sup> These physiological abnormalities make transvascular transport—movement from vessels to the interstitium—and interstitial transport—movement through the interstitium to target cells—heterogeneous.<sup>[4a]</sup> Hence the tumor microenvironment limits the uniform penetration of nanotherapeutics by slowing or halting their transport through hydrodynamic and steric hindrance.<sup>[2a,3a,5]</sup> Overcoming these physiological barriers in tumors is an outstanding challenge for nanomedicine.

Rational design of nanotherapeutic physicochemical properties can optimize tumor penetration by circumventing these barriers. Decreasing nanoparticle size improves delivery to some degree, leading to longer circulation times<sup>[4c]</sup> and more rapid transport within tumors,<sup>[4b,c]</sup> yet smaller nanoparticles have lower drug payloads and loading efficiencies. The role of surface charge is similarly complex; cationic charge optimizes transvascular transport in tumors<sup>[6]</sup> while neutral charge is ideal for long circulation times<sup>[7]</sup> and interstitial transport in tumors,<sup>[8]</sup> making charge unattractive

to modulate. Particle aspect ratio can also affect diffusion rates through pores and porous media,<sup>[9]</sup> but the effects of aspect ratio on tumor penetration are not known. We hypothesized that nanorods, through enhanced transport across porous media, would penetrate tumors more efficiently than nanospheres of the same effective hydrodynamic size.

To test this hypothesis, we studied whether nanospheres and nanorods with the same diffusive transport rates in water would transport at different rates in porous media and tumors. To this end, we designed and developed biostable colloidal quantum dot-based nanospheres and nanorods that have tunable size but identical surface coating and charge (Figure 1). The spectrally distinct fluorescence from the quantum dot cores in both these nanoparticles (Supporting Information, Figure S1) allowed for real-time multiplexed in vivo imaging with multiphoton microscopy within the same tumor. Applying this technology, we measured transport in vitro and in vivo for a pair of nanospheres and nanorods with equal hydrodynamic size.

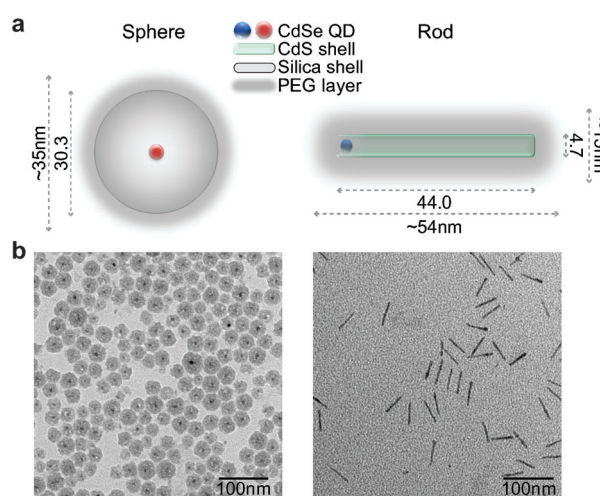


**Figure 1.** Nanospheres and nanorods designed for real-time in vivo imaging. a) Schematic representation of nanospheres and nanorods. The PEG layer is depicted as a gray glow. Dimensions obtained with TEM for the nanorod cores are shown (4.7 nm diameter and 44.0 nm length) as well as the approximate PEG-coated hydrodynamic lengths (15 nm diameter and 54 nm length). The hydrodynamic diameter range of the nanospheres and nanorods (obtained with DLS) is also shown (33–35 nm). b) TEM images of nanospheres and nanorods.

We used recently developed polyethylene glycol-modified (PEG) CdSe/CdS quantum-dot cores with spherical silica shells for the nanospheres<sup>[4c]</sup> and CdSe quantum-dot cores

[\*] V. P. Chauhan,<sup>[†]</sup> Prof. Dr. D. Fukumura, Prof. Dr. R. K. Jain  
Edwin L. Steele Laboratory, Department of Radiation Oncology  
Massachusetts General Hospital and Harvard Medical School  
100 Blossom St., Boston, MA 02114 (USA)  
E-mail: jain@steele.mgh.harvard.edu

Dr. Z. Popović,<sup>[†]</sup> Dr. O. Chen, J. Cui, Prof. Dr. M. G. Bawendi  
Department of Chemistry, Massachusetts Institute of Technology  
77 Massachusetts Ave., Cambridge MA 02139 (USA)  
E-mail: mgb@mit.edu

V. P. Chauhan<sup>[†]</sup>  
Harvard School of Engineering and Applied Sciences  
Harvard University (USA)

[†] These authors contributed equally to this work.

[\*\*] We thank Debby Pheasant (BIF Facility, MIT), Julia Kahn (MGH), and Sylvie Roberge (MGH) for technical assistance. This research was supported by the U.S. National Cancer Institute grants R01-CA126642 (R.K.J. and M.G.B.), R01-CA085140, R01-CA115767 (R.K.J.), P01-CA080124 (R.K.J. and D.F.), R01-CA096915 (D.F.); by the U.S. Department of Defense Breast Cancer Research Program Innovator Award W81XWH-10-1-0016 (R.K.J.); by the MIT-Harvard NIH Center for Cancer Nanotechnology Excellence 1U54-CA119349 (M.G.B.); by the MIT DCIF CHE-980806, DBI-9729592; by the ISN W911NF-07-D-0004 (M.G.B.); by the NSF-MRSEC program (DMR-0117795) via the use of its shared user facilities.

Supporting information for this article is available on the WWW under <http://dx.doi.org/10.1002/anie.201104449>.

with seed-grown elongated CdS shells<sup>[10]</sup> capped with a PEG layer for the nanorods. The synthetic procedures for silica coating and PEG capping were adapted from the literature.<sup>[11]</sup> Unlike for the case of spherical nanoparticles, aqueous solutions of stable and uniform CdSe/CdS nanorods are difficult to obtain. Only longer PEG chains (MW 5000) provided aqueous solutions of nanorods that could satisfy multiple criteria for in vivo imaging.<sup>[4c]</sup> To determine the rod dimensions—including hydrodynamic aspect ratio—with PEG, we measured the thickness of the PEG layer based on inter-rod packing distances with and without PEG using transmission electron microscopy (TEM). We found this layer to be approximately 5 nm, and confirmed the measurement by comparing the difference between the hydrodynamic and inorganic sizes for spherical nanoparticles with the same PEG coating (Figure S2 and Table S1). We then tested the particles for stability and serum adsorption at 37 °C by incubating them in phosphate-buffered saline (PBS) and fetal bovine serum (FBS), respectively. We found that both were stable and maintained their hydrodynamic size in serum (Figure S3, S4) as expected for PEG coated particles,<sup>[12]</sup> though we could not exclude the formation of a small protein corona.<sup>[13]</sup> We estimated particle surface charge by measuring  $\zeta$ -potentials, which were  $-5.9 \pm 4.0$  mV<sup>[4c]</sup> and  $-4.9 \pm 6.2$  mV for the nanospheres and nanorods respectively (Figure S5).

To determine if nanorods would transport through porous media more rapidly than nanospheres of the same hydrodynamic size, we compared 15 nm diameter by 54 nm length rods with 35 nm diameter spheres. Both had a 33–35 nm hydrodynamic diameter, measured by dynamic light scattering (DLS) and fluorescence correlation spectroscopy, and therefore had nearly identical diffusion rates in water (Table S2). We then measured transport for both particles across porous membranes in vitro<sup>[9a]</sup> with pore diameters from 100–5000 nm (Figure 2a). While both the nanospheres and nanorods diffused through 5000 nm pores at the same rate, the nanorods passed through 100–400 nm pores—in the range of maximum pore sizes in tumor vascular walls<sup>[2a]</sup>—up to an order of magnitude faster than the nanospheres. Next, we tested transport through tumor-mimetic collagen gels<sup>[3a]</sup> for both particles, and found that the nanorods diffused through

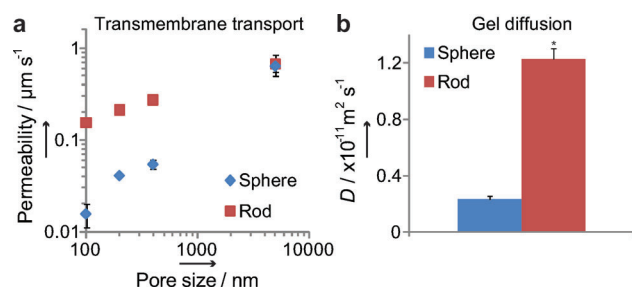


**Figure 2.** Transport rates in vitro for nanospheres versus nanorods of the same hydrodynamic diameter (33–35 nm). a) Diffusion rates across membranes with varied pore size, quantified as permeability. Both particles pass through micrometer-range pores at the same rate, while nanometer-range pores hinder the nanospheres more than the nanorods. b) Diffusion coefficients in 1% collagen gels. The nanorods diffuse 5.3-times as fast as the nanospheres ( $p=0.003$ , \*).

these gels 5.3 times as fast as the nanospheres (Figure 2b;  $p=0.003$ , Student's T-test,  $n=3$ ).

Considering their superior transport through porous media in vitro, we tested to see if the nanorods could penetrate tumors more effectively than the nanospheres in vivo. We intravenously co-injected the same two 33–35 nm hydrodynamic diameter particles—bearing different emission maxima—into female SCID mice bearing orthotopic E0771 mammary tumors in mammary fat pad windows,<sup>[14]</sup> and then intravitally imaged their penetration in these tumors over time using multiphoton microscopy. We quantified nanoparticle transvascular transport as transvascular mass flux per unit vascular surface area and transvascular concentration difference (Figure 3a), also referred to as the effective permeability.<sup>[15]</sup> We found that the nanorods penetrated tumors 4.1 times as rapidly as the nanospheres ( $p=0.03$ , Student's T-test,  $n=6$ ).

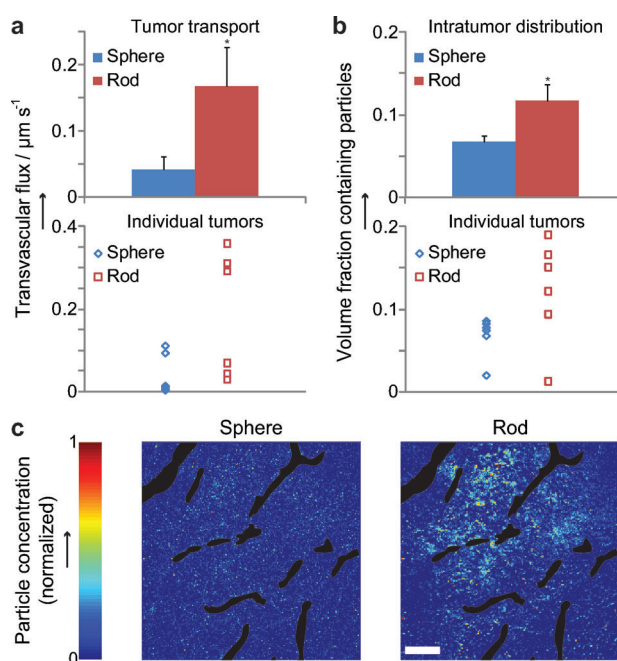


**Figure 3.** Transport and distribution in tumors in vivo for nanospheres versus nanorods of the same hydrodynamic diameter (33–35 nm).

a) Transvascular transport rates in orthotopic E0771 mammary tumors in mice. The nanorods are transported across vessel walls 4.1-times as fast as the nanospheres ( $p=0.03$ , \*). b) Nanoparticle distribution in orthotopic E0771 mammary tumors in mice. The nanorods penetrate to 1.7 times the volume to which the nanospheres distribute ( $p=0.01$ , \*). c) Nanoparticle penetration in tumors. Intensities are normalized to initial intravascular levels, and vessels are shown in black. The rods extravasate more and penetrate deeper than the spheres. Scale bar 100  $\mu\text{m}$ .

We further measured nanoparticle distribution—a consequence of interstitial transport—throughout tumors 1 h after injection (Figure 3b,c), quantified as the extravascular volume fraction of each tumor that contained nanoparticles. We determined that the nanorods penetrated to 1.7 times the volume to which the nanospheres distributed at 1 h post-injection ( $p=0.01$ , Student's T-test,  $n=6$ ). Importantly these

particles showed no difference in plasma half-life in non-tumor bearing mice (Figure S6), indicating similar uptake and clearance rates by the organs. We additionally found that these 14 nm diameter 55 nm length nanorods transported into E0771 tumors nearly as rapidly as 13 nm diameter PEG-coated CdSe/CdS quantum dots (Figure S7), suggesting that the short dimension for nanorods largely determines transport rates across pores.

It is important to consider that even small improvements in nanotherapeutic penetration can result in significant enhancements to therapeutic effectiveness. Preventing matrix production in tumors with losartan, which improves probe diffusion rates by a factor of 1.6 and nanoparticle distribution in tumors by a factor of 2, can more than double the effectiveness of an oncolytic virus or nanoparticle therapy against tumor growth.<sup>[16]</sup> Similarly, degrading tumor collagen with collagenase, which improves probe diffusion rates<sup>[3b]</sup> by a factor of 1.75–2 and virus distribution<sup>[5b]</sup> by a factor of 3, can more than triple the effectiveness of an oncolytic virus against tumor growth.<sup>[5d]</sup> Finally, repairing abnormal tumor blood vessel function through vascular normalization with anti-angiogenic agents, which improves probe penetration in tumors<sup>[17]</sup> by a factor of 1.5, has shown great promise for improving small-molecule chemotherapeutic effectiveness in preclinical and clinical studies.<sup>[18]</sup> A meaningful comparison of nanosphere versus nanorod therapeutic effectiveness may prove intractable due to the need to match size, charge, surface chemistry, drug loading, and release kinetics. Still, considering historical data on the connection between transport rates and therapeutic effectiveness, our results strongly suggest that nanorods will be more effective drug carriers than nanospheres for anti-cancer therapy.

Our data show that nanoparticle shape is an important property to be explored for the design of effective nanomedicine. Combining the in vitro and in vivo results, in which the differences in transport rates are similar, it is likely that nanorods penetrate tumors more rapidly than nanospheres due to improved transport through pores. Other mechanisms, such as alignment with bloodflow increasing the probability of convective delivery for nanorods,<sup>[19]</sup> are very unlikely since tumors tend to have sluggish blood flow and low transvascular fluid flux.<sup>[4a]</sup> We therefore speculate that reduced steric hindrance from and viscous drag near vessel pore walls leads to the difference in nanosphere versus nanorod delivery, as seems to be the case for transport across membranes with uniform pores in vitro.<sup>[9a]</sup> Interestingly, flexible nanorods may be able to take greater advantage of this mechanism, as they demonstrate reptation behavior that improves their transport versus rigid rods through porous gels.<sup>[9b]</sup> Flexible rods also demonstrate superior circulation times when compared to rigid rods, likely through enhanced evasion of phagocytosis.<sup>[20]</sup> Furthermore, nanorods feature a larger surface/volume ratio than nanospheres, which may prove advantageous since the addition of a targeting ligand can aid in cell binding, cell uptake, and therapeutic effectiveness.<sup>[21]</sup> Considering these superior properties, it seems that rod shaped nanotherapeutics—including nanotubes and nanoworms—may be far more effective for cancer therapy than the currently approved spherical nanomedicines.

Received: June 27, 2011  
Revised: August 16, 2011  
Published online: October 6, 2011

**Keywords:** cancer · imaging agents · luminescence · microscopy · nanoparticles

- [1] a) D. Peer, J. M. Karp, S. Hong, O. C. Farokhzad, R. Margalit, R. Langer, *Nat. Nanotechnol.* **2007**, *2*, 751; b) V. P. Torchilin, *Nat. Rev. Drug Discovery* **2005**, *4*, 145.
- [2] a) S. K. Hobbs, W. L. Monsky, F. Yuan, W. G. Roberts, L. Griffith, V. P. Torchilin, R. K. Jain, *Proc. Natl. Acad. Sci. USA* **1998**, *95*, 4607; b) F. Yuan, M. Leunig, S. K. Huang, D. A. Berk, D. Papahadjopoulos, R. K. Jain, *Cancer Res.* **1994**, *54*, 3352.
- [3] a) V. P. Chauhan, R. M. Lanning, B. Diop-Frimpong, W. Mok, E. B. Brown, T. P. Padera, Y. Boucher, R. K. Jain, *Biophys. J.* **2009**, *97*, 330; b) P. A. Netti, D. A. Berk, M. A. Swartz, A. J. Grodzinsky, R. K. Jain, *Cancer Res.* **2000**, *60*, 2497.
- [4] a) V. P. Chauhan, T. Stylianopoulos, Y. Boucher, R. K. Jain, *Annu. Rev. Chem. Biomol. Eng.* **2011**, *2*, 281; b) A. Pluen, Y. Boucher, S. Ramanujan, T. D. McKee, T. Gohongi, E. di Tomaso, E. B. Brown, Y. Izumi, R. B. Campbell, D. A. Berk, R. K. Jain, *Proc. Natl. Acad. Sci. USA* **2001**, *98*, 4628; c) Z. Popović, W. Liu, V. P. Chauhan, J. Lee, C. Wong, A. B. Greytak, N. Insin, D. G. Nocera, D. Fukumura, R. K. Jain, M. G. Bawendi, *Angew. Chem.* **2010**, *122*, 8831; *Angew. Chem. Int. Ed.* **2010**, *49*, 8649.
- [5] a) E. R. Weeks, T. Gisler, P. D. Kaplan, D. A. Weitz, *Phys. Rev. Lett.* **2000**, *85*, 888; b) W. M. Deen, *AIChE J.* **1987**, *33*, 1409; c) T. G. Mason, K. Ganesan, J. H. van Zanten, D. Wirtz, S. C. Kuo, *Phys. Rev. Lett.* **1997**, *79*, 3282; d) T. D. McKee, P. Grandi, W. Mok, G. Alexandrakos, N. Insin, J. P. Zimmer, M. G. Bawendi, Y. Boucher, X. O. Breakefield, R. K. Jain, *Cancer Res.* **2006**, *66*, 2509.
- [6] a) R. B. Campbell, D. Fukumura, E. B. Brown, L. M. Mazzola, Y. Izumi, R. K. Jain, V. P. Torchilin, L. L. Munn, *Cancer Res.* **2002**, *62*, 6831; b) M. Dellian, F. Yuan, V. S. Trubetsky, V. P. Torchilin, R. K. Jain, *Br. J. Cancer* **2000**, *82*, 1513.
- [7] A. L. Klibanov, K. Maruyama, V. P. Torchilin, L. Huang, *FEBS Lett.* **1990**, *268*, 235.
- [8] T. Stylianopoulos, M. Z. Poh, N. Insin, M. G. Bawendi, D. Fukumura, L. L. Munn, R. K. Jain, *Biophys. J.* **2010**, *99*, 1342.
- [9] a) W. M. Deen, M. P. Bohrer, N. B. Epstein, *AIChE J.* **1981**, *27*, 952; b) A. Pluen, P. A. Netti, R. K. Jain, D. A. Berk, *Biophys. J.* **1999**, *77*, 542.
- [10] a) L. Carbone, C. Nobile, M. De Giorgi, F. D. Sala, G. Morello, P. Pompa, M. Hytch, E. Snoeck, A. Fiore, I. R. Franchini, M. Nadasan, A. F. Silvestre, L. Chiodo, S. Kudera, R. Cingolani, R. Krahne, L. Manna, *Nano Lett.* **2007**, *7*, 2942; b) D. V. Talapin, J. H. Nelson, E. V. Shevchenko, S. Aloni, B. Sadtlir, A. P. Alivisatos, *Nano Lett.* **2007**, *7*, 2951.
- [11] a) M. D. Butterworth, L. Illum, S. S. Davis, *Colloids Surf. A* **2001**, *179*, 93; b) R. Koole, M. M. van Schooneveld, J. Hilhorst, C. D. Donega, D. C. t'Hart, A. van Blaaderen, D. Vanmaekelbergh, A. Meijerink, *Chem. Mater.* **2008**, *20*, 2503.
- [12] R. Gref, A. Domb, P. Quellec, T. Blunk, R. H. Müller, J. M. Verbavatz, R. Langer, *Adv. Drug Delivery Rev.* **1995**, *16*, 215.
- [13] a) I. Lynch, K. A. Dawson, *Nano Today* **2008**, *3*, 40; b) C. Röcker, M. Pötzl, F. Zhang, W. J. Parak, G. U. Nienhaus, *Nat. Nanotechnol.* **2009**, *4*, 577.
- [14] B. J. Vakoc, R. M. Lanning, J. A. Tyrrell, T. P. Padera, L. A. Bartlett, T. Stylianopoulos, L. L. Munn, G. J. Tearney, D. Fukumura, R. K. Jain, B. E. Bouma, *Nat. Med.* **2009**, *15*, 1219.
- [15] E. B. Brown, R. B. Campbell, Y. Tsuzuki, L. Xu, P. Carmeliet, D. Fukumura, R. K. Jain, *Nat. Med.* **2001**, *7*, 864.

- [16] B. Diop-Frimpong, V. P. Chauhan, S. Krane, Y. Boucher, R. K. Jain, *Proc. Natl. Acad. Sci. USA* **2011**, *108*, 2909.
  - [17] R. T. Tong, Y. Boucher, S. V. Kozin, F. Winkler, D. J. Hicklin, R. K. Jain, *Cancer Res.* **2004**, *64*, 3731.
  - [18] R. K. Jain, D. G. Duda, J. W. Clark, J. S. Loeffler, *Nat. Clin. Pract. Oncol.* **2006**, *3*, 24.
  - [19] A. Ruggiero, C. H. Villa, E. Bander, D. A. Rey, M. Bergkvist, C. A. Batt, K. Manova-Todorova, W. M. Deen, D. A. Scheinberg, M. R. McDevitt, *Proc. Natl. Acad. Sci. USA* **2010**, *107*, 12369.
  - [20] Y. Geng, P. Dalhaimer, S. Cai, R. Tsai, M. Tewari, T. Minko, D. E. Discher, *Nat. Nanotechnol.* **2007**, *2*, 249.
  - [21] J. H. Park, G. von Maltzahn, L. Zhang, A. M. Derfus, D. Simberg, T. J. Harris, E. Ruoslahti, S. N. Bhatia, M. J. Sailor, *Small* **2009**, *5*, 694.
-